

Journal Pre-proof

ATP2B2 de novo variants as a cause of variable neurodevelopmental disorders that feature dystonia, ataxia, intellectual disability, behavioral symptoms, and seizures

Elena Poggio, Lucia Barazzuol, Andrea Salmaso, Celeste Milani, Adamantia Deligiannopoulou, Ángeles García Cazorla, Se Song Jang, Natalia Juliá-Palacios, Boris Keren, Robert Kopajtich, Sally Ann Lynch, Cyril Mignot, Catherine Moorwood, Christiane Neuhofer, Vincenzo Nigro, Anna Oostra, Holger Prokisch, Virginie Saillour, Nika Schuermans, Annalaura Torella, Patrick Verloo, Elise Yazbeck, Marcella Zollino, Robert Jech, Juliane Winkelmann, Jan Neczal, Tito Cali, Marisa Brini, Michael Zech



PII: S1098-3600(23)00987-5

DOI: <https://doi.org/10.1016/j.gim.2023.100971>

Reference: GIM 100971

To appear in: *Genetics in Medicine*

Received Date: 12 May 2023

Revised Date: 28 August 2023

Accepted Date: 29 August 2023

Please cite this article as: Poggio E, Barazzuol L, Salmaso A, Milani C, Deligiannopoulou A, Cazorla ÁG, Jang SS, Juliá-Palacios N, Keren B, Kopajtich R, Lynch SA, Mignot C, Moorwood C, Neuhofer C, Nigro V, Oostra A, Prokisch H, Saillour V, Schuermans N, Torella A, Verloo P, Yazbeck E, Zollino M, Jech R, Winkelmann J, Neczal J, Cali T, Brini M, Zech M, *ATP2B2 de novo* variants as a cause of variable neurodevelopmental disorders that feature dystonia, ataxia, intellectual disability, behavioral symptoms, and seizures, *Genetics in Medicine* (2023), doi: <https://doi.org/10.1016/j.gim.2023.100971>.

This is a PDF file of an article that has undergone enhancements after acceptance, such as the addition of a cover page and metadata, and formatting for readability, but it is not yet the definitive version of record. This version will undergo additional copyediting, typesetting and review before it is published in its final form, but we are providing this version to give early visibility of the article. Please note that, during the production process, errors may be discovered which could affect the content, and all legal disclaimers that apply to the journal pertain.

© 2023 Published by Elsevier Inc. on behalf of American College of Medical Genetics and Genomics.

***ATP2B2 de novo* variants as a cause of variable neurodevelopmental disorders that feature dystonia, ataxia, intellectual disability, behavioral symptoms, and seizures**

Elena Poggio^{1,§}, Lucia Barazzuo^{2,§}, Andrea Salmaso^{1,§}, Celeste Milani¹, Adamantia Deligiannopoulou², Ángeles García Cazorla^{3,4,5}, Se Song Jang⁶, Natalia Juliá-Palacios⁷, Boris Keren⁸, Robert Kopajtich^{9,10}, Sally Ann Lynch¹¹, Cyril Mignot⁸, Catherine Moorwood¹², Christiane Neuhofer^{9,10}, Vincenzo Nigro¹³, Anna Oostra¹⁴, Holger Prokisch^{9,10}, Virginie Saillour¹⁵, Nika Schuermans^{16,17}, Annalaura Torella¹³, Patrick Verloo¹⁸, Elise Yazbeck¹⁹, Marcella Zollino²⁰, Robert Jech²¹, Juliane Winkelmann^{9,10,22}, Jan Ncnpa^{23,24}, Tito Cali^{2,25,26,#}, Marisa Brini^{1,25,#}, Michael Zech^{9,10,27,#}*

§These authors contributed equally to this work as first authors.

#These authors contributed equally to this work as last authors.

¹Department of Biology, University of Padua, Padua, Italy

²Department of Biomedical Sciences, University of Padua, Padua, Italy

³European Reference Network for Hereditary Metabolic Diseases (MetabERN)

⁴Neurometabolic Unit and Synaptic Metabolism Laboratory, Neurology Department Sant Joan de Déu Hospital, IPR, Barcelona, Spain

⁵Centro de Investigación Biomédica en Red de Enfermedades Raras (CIBERER), Instituto de Salud Carlos III, Madrid, Spain

⁶Seoul National University (SNU) College of Medicine, Seoul, South Korea

⁷Neurology Department, Neurometabolic Unit, Institut de Recerca, CIBERER and MetabERN, Hospital Sant Joan de Déu, Barcelona, Spain

⁸APHP.Sorbonne Université, Department of Medical Genetics, Pitié-Salpêtrière University Hospital, Paris, France and Centre de Référence Maladies Rares Déficiences Intellectuelles de Causes Rares

⁹Institute of Neurogenomics, Helmholtz Zentrum München, Munich, Germany

¹⁰Institute of Human Genetics, School of Medicine, Technical University of Munich, Munich, Germany

¹¹Department of Clinical Genetics, Temple Street Children's University Hospital, Dublin, Ireland

¹²Exeter Genomics Laboratory, Royal Devon University Healthcare NHS Foundation Trust, Exeter, United Kingdom

¹³Department of Precision Medicine, University of Campania, Luigi Vanvitelli, Napoli, Italy

¹⁴Department of Pediatrics, Division of Pediatric Neurology and Metabolism, Ghent University Hospital, Ghent, Belgium

¹⁵Laboratoire de biologie médicale multisites Sequoia - FMG2025, Paris, France

¹⁶Center for Medical Genetics Ghent, Ghent University Hospital, Ghent, Belgium

¹⁷Department of Biomolecular Medicine, Ghent University Hospital, Ghent, Belgium

¹⁸Department of Pediatric Neurology, Center for Inherited Metabolic Disorders and metabERN, University Hospital Ghent, Ghent, Belgium

¹⁹Pediatric Neurology Department, Assistance Publique-Hôpitaux de Paris, Hôpitaux Universitaires Paris Saclay, Bicêtre Hospital, Le Kremlin Bicêtre, France

²⁰Unit of Medical Genetics, Section of Genomic Medicine, Department of Life Sciences and Public Health, Università Cattolica del Sacro Cuore, Fondazione Policlinico Universitario A. Gemelli IRCCS, Rome, Italy

²¹Department of Neurology, Charles University in Prague, 1st Faculty of Medicine and General University Hospital in Prague, Prague, Czech Republic

²²Munich Cluster for Systems Neurology, SyNergy, 81377 Munich, Germany

²³2nd Department of Neurology, Faculty of Medicine, Comenius University, Bratislava, Slovakia

²⁴Department of Neurology, Zvolen Hospital, Zvolen, Slovakia

²⁵Centro Studi per la Neurodegenerazione (CESNE), University of Padua, Padua, Italy

²⁶Neuroscience Center (PNC), University of Padua, Padua, Italy

²⁷Institute for Advanced Study, Technical University of Munich, Lichtenbergstrasse 2a, 85748 Garching, Germany

*Correspondence to:

PD Dr. Michael Zech, Institute of Neurogenomics, Helmholtz Zentrum München
Deutsches Forschungszentrum für Gesundheit und Umwelt (GmbH)

Ingolstädter Landstraße 1

85764 Neuherberg, Germany

E-mail: michael.zech@mri.tum.de

Phone: 0049-89-3187-1884

Fax: 0049-89-3187-3297

Abstract

Purpose: *ATP2B2* encodes the variant-constrained plasma-membrane calcium-transporting ATPase-2, expressed in sensory ear cells and specialized neurons. *ATP2B2/Atp2b2* variants were previously linked to isolated hearing loss in patients and neurodevelopmental deficits with ataxia in mice. We aimed to establish the association between *ATP2B2* and human neurological disorders.

Methods: Multinational case recruitment, scrutiny of trio-based genomics data, *in-silico* analyses, and functional variant characterization were performed.

Results: We assembled seven individuals harboring rare, predicted deleterious heterozygous *ATP2B2* variants. The alleles comprised five missense substitutions affecting evolutionarily conserved sites and two frameshift variants in the penultimate exon. For six variants, a *de-novo* status was confirmed. Unlike described patients with hearing loss, the individuals displayed a spectrum of neurological abnormalities, ranging from ataxia with dystonic features to complex neurodevelopmental manifestations with intellectual disability, autism, and seizures. Two cases with recurrent amino-acid variation showed distinctive overlap with cerebellar atrophy-associated ataxia and epilepsy. In cell-based studies, all variants caused significant alterations in cytosolic calcium handling with both loss- and gain-of-function effects.

Conclusion: Presentations in our series recapitulate key phenotypic aspects of *Atp2b2*-mouse models and underline the importance of precise calcium regulation for neurodevelopment and cerebellar function. Our study documents a role for *ATP2B2* variants in causing heterogeneous neurodevelopmental and movement-disorder syndromes.

Keywords

Plasma membrane Ca^{2+} ATPase isoform 2, *ATP2B2*, ataxia, neurodevelopmental disorder

Introduction

Deregulation of Ca^{2+} homeostasis is poorly compensated in neurons and linked to various cognitive, behavioral, sensory, and movement disorders in mice and humans^{1,2}. A specialized system of energy-dependent active transporters is crucially involved in the control of intracellular Ca^{2+} concentrations, the plasma membrane Ca^{2+} ATPases (PMCA)³. These transmembrane pumps export Ca^{2+} from all eukaryotic cells and function as critical gatekeepers of the Ca^{2+} handling machinery in diverse organs including the brain, where they are required for synapse biogenesis, plasticity, and prevention of neuronal loss⁴. In the mammalian genome, different PMCA isoforms (*ATP2B1-4*) are the products of four genes, namely *ATP2B1*, *ATP2B2*, *ATP2B3*, and *ATP2B4*⁴. PMCA share a common structure of ten membrane-spanning segments, two intracellular loop domains (between transmembrane regions 2-3 and 4-5) responsible for autoinhibitory and catalytic mechanisms, and N- and C-terminal cytoplasmic tails^{4,5}. The C-tail mediates the ability of PMCA to interact with calmodulin, the major regulatory protein affecting pump activity; binding of calmodulin to its domain in PMCA's C-terminus alters Ca^{2+} clearance rates and fine-tuning of signal transmission by changing intrinsic protein conformations that maintain the pump in an autoinhibited state^{3,6}. Although PMCA are ubiquitous enzymes in human cells, the four isoforms are distributed in a tissue-specific manner and undergo distinct expression regulation during development and differentiation⁷. *ATP2B1* and *ATP2B4* are present in virtually all tissues, including most brain regions, whereas *ATP2B2* and *ATP2B3* are highly enriched in some specialized populations of neuronal and excitable cells⁷. *ATP2B2* is predominantly found in Purkinje and granular neurons of the

cerebellum as well as presynaptic terminals of the forebrain, but also abundant in sensory cells of the cochlear and vestibular systems^{3,7}. The variable abundance in certain neuroanatomical structures and the cell type-specificity of separate PMCA isoforms suggests that these pumps are exquisitely adapted for performing Ca^{2+} exports in the context of local physiological requirements, perturbations of which may lead to spatially defined Ca^{2+} signaling defects and specific human disease traits⁸. Consistent with this, mutational changes of three PMCA-encoding genes have been associated with OMIM-listed monogenic disorders, all of which present with neurological and/or sensory impairments⁹. Heterozygous *ATP2B1* *de novo* missense substitutions and protein-truncating variants (PTVs) underlie variable neurodevelopmental diseases with developmental delay, intellectual disability, behavioral problems, and seizures (MIM:619910)¹⁰, whereas X-linked missense variants in *ATP2B3* produce ataxia and ataxia-dystonia phenotypes (MIM:302500)^{11,12}. Recently, heterozygous PTVs of *ATP2B2*, including two *de novo* variants, have been detected in five families with isolated non-syndromic hearing loss¹³, resulting in association of *ATP2B2* to autosomal dominant deafness-82 (MIM:619804). Based on *ATP2B2*'s predicted intolerance to PTVs (gnomAD pLI score = 1.0; observed/expected ratio = 0.06, CI = 0.03-0.15)¹⁴ and the location of identified variants, haploinsufficiency has been proposed as the most likely pathogenic mechanism causing the deafness manifestations in affected individuals¹³. However, *ATP2B2* missense substitutions are also markedly underrepresented compared to expectation in gnomAD (missense z score = 4.55; observed/expected ratio = 0.54, CI = 0.5-0.59)¹⁴, indicating that additional variant alleles and/or molecular effects different from simple heterozygous loss of *ATP2B2* may contribute to clinical disease presentations. Our group has described previously one single individual affected by ataxia and comorbid intellectual deficits without hearing impairment who was identified to have a rare *ATP2B2* missense

variant of undetermined inheritance and uncertain clinical significance¹⁵; the pathological impact of mutant *ATP2B2* in neurodevelopmental disease remained elusive until today.

Here, we report on a multinational collaboration, facilitated by GeneMatcher¹⁶, which led to identification of heterozygous, mostly *de novo* *ATP2B2* missense and frameshift variants (the latter situated in the penultimate exon) in seven individuals with movement disorders and neurodevelopmental phenotypes. One amino acid substitution was recurrent in two patients. Hearing impairment was documented in only two cases, in whom it represented a minor feature compared to observed neurodevelopmental disturbances. We demonstrate Ca^{2+} extrusion dysfunction for variant-bearing proteins in experimental assays. Our findings significantly broaden the genotypic and phenotypic spectrum of *ATP2B2*-related diseases and provide further impetus for the continued elucidation of the role of PMCA in neurotypical development and cerebellar function.

Materials and Methods

Human genetics and patient series recruitment

To uncover the genetic causes of their illnesses, all affected individuals presented in this study were exome-sequenced. Parent-child trio analyses were performed in six families (individuals 1-6; for individual 1 complementary trio genome sequencing was also performed), whereas individual 7 was sequenced together with the unaffected mother (paternal DNA sample unavailable). Genetic investigations, variant discovery, and gene prioritization procedures were carried out as described before¹⁷⁻²³. We first singled out a novel heterozygous *ATP2B2* *de novo* missense substitution as the sole suspicious finding in a Slovak research proband (individual 1) who was part of a large local cohort of patients with dystonic phenotypes including dystonia-ataxia syndromes

and neurodevelopmental disorders with dystonia (Munich, Germany)^{17,24}. Candidate *ATP2B2* variants were next queried in online matchmaking catalogues¹⁶ and in-house genomic data collections²³. Our searches led to ascertainment of an additional six patients suspected of having undiagnosed monogenic phenotypes (individuals 2-6 from GeneMatcher¹⁶; individual 7 from our private database in Munich, Germany), for whom exome-wide testing had prioritized mutational changes of *ATP2B2* and excluded pathogenic or likely pathogenic variants²⁵ in any known disease-associated genes. These individuals were all evaluated for medical complexity with congenital severe neurological involvement and identified from rare-disease clinical research programs in Italy, UK, Belgium, South Korea, France, and Spain. All herein reported variants were annotated based on *ATP2B2*'s canonical transcript RefSeq: NM_001001331.4 (GENECODE: ENST00000360273). The clinical assessment of affected individuals included (neuro)imaging and electroencephalographic studies as appropriate, physical examinations, and review of lifetime medical records; most patients had extensive unyielding routine diagnostic testing results including normal chromosomal microarray analysis. Informed consent was obtained from adult patients or legal representatives in case of children for each participant of this study.

In-silico missense variant analysis

Protein modeling was undertaken as previously described²⁶. Structural models of wild-type and mutant *ATP2B2* pumps in the Ca²⁺-free state were generated with the Alpha-Fold Software by using the Q01814 (AT2B2_HUMAN) entry. Obtained structures were assessed by using Pymol.

Site-directed mutagenesis

ATP2B2 cDNAs of human origin were used as targets, as described^{15,26}. Site-directed mutagenesis on cDNA templates was carried out according to the manufacturer's recommendations (QuickChange XL site-direct mutagenesis kit, Agilent). Primer sequences are available upon request. Each construct was verified by direct sequencing.

Cell culture and transfection

HeLa cells were cultured according to standard procedures¹⁵; 12 h before transfection, cells were seeded onto 13-mm glass coverslips (immunocytochemistry analysis) or 6-multiwell plates (Western blotting and aequorin Ca^{2+} measurements). Transfections were performed as detailed earlier¹⁵. For the Ca^{2+} transport studies, co-transfections with the aequorin construct (cytAEQ) and the empty vector (mock) or ATP2B2-expressing plasmids were conducted. The cytAEQ expression plasmid has been described elsewhere¹⁵.

Western blotting and immunolocalization

Western blot and immunocytochemistry studies on HeLa cells overexpressing wild-type and mutant ATP2B2 pumps were performed as described in Vicario et al¹⁵. The monoclonal anti-PMCA clone 5F10 (1:1,000; Thermo Scientific, catalog#MA3-914; directed against amino acids 702-761 in ATP2B2) and monoclonal anti-actin (1:1000; Thermo Scientific, catalog#MA1-744) were used as primary antibodies; the HRP-conjugated goat anti-mouse was used as secondary antibody (1:50000; Sigma Aldrich catalog#A9044). The signal was revealed by the incubation with Luminata Classico HRP substrate (Merck Millipore; WBLUO500). The bioluminescence signal was detected with the ChemiDoc Imaging System (Biorad). The built-in software detects the signal in "Preview" mode and, then, automatically adjusts the acquisition settings

to avoid saturated signals. The densitometric analysis was performed on an image obtained by the average of at least three different acquisitions with increasing exposure time and analyzed by the Fiji software (NIH software). The region of interest corresponding to each band was defined manually and the densitometry of each band was automatically measured by the Gel analyzer plugin. The same procedure was performed for both the PMCA and actin signals. For each sample, the densitometry value of PMCA was normalized to the actin value.

Ca²⁺ measurements with recombinant aequorin

Determination of cytosolic Ca²⁺ concentrations in transfected HeLa cells (cytAEQ) was performed in a Perkin-Elmer Envision plate reader equipped with a two-injectors unit. Measurements and calibrations of aequorin signals were carried out as previously described¹⁵. Briefly, transfected cytAEQ was reconstituted by incubating the cells for 1–3 h with 5 μ M coelenterazine wt in KRB at 37°C. The experiments were terminated by lysing the cells with 100 μ M digitonin in a hypotonic Ca²⁺-rich solution (10 mM CaCl₂ in H₂O) to discharge the remaining aequorin pool after histamine stimulation. The light signal was collected and calibrated into [Ca²⁺]_{cyt} values as previously reported^{27,28}. The calibration protocol takes into consideration the amount of aequorin discharged each second (L) over a value L_{max}, corresponding to the total reconstituted and active aequorin determined for each measurement at the end of the experiment by exposing the cells to 10 mM CaCl₂ in H₂O. This protocol overcomes possible differences related to the amount of expressed probe or to reconstitution with the prosthetic group coelenterazine. Output data were reported as means \pm SEM. Statistical differences were calculated by One-Way-ANOVA test; *p*-values of ≤ 0.05 were considered statistically significant.

Results

Variant spectrum

We ascertained seven unrelated individuals, from nonconsanguineous families of various geographical origins, who carried heterozygous variants in *ATP2B2* and presented overlapping phenotypes that differed from those associated with previously reported PTVs of this gene¹³ (**Tab.1**, **Fig.1A-C**). None of the *ATP2B2* variants identified were present in population controls (gnomAD, v2.1 and v3.1 releases) or in-house control datasets at the participating centers. Individuals 1-4 had *de novo* missense variants: c.3028G>A, p.(Glu1010Lys); c.2511G>T, p.(Met837Ile); c.2633T>C, p.(Phe878Ser); c.358G>A, p.(Gly120Arg), and a fifth patient (individual 7) had another nucleotide substitution at cDNA position 358 (c.358G>C) resulting in the same missense amino acid change as seen in individual 4, namely p.(Gly120Arg). For individual 7, a *de novo* status of the variant could not be confirmed due to unavailability of genetic material from the father (variant absent in the mother's DNA). The variant effect evaluation tool CADD predicted the variants to be highly deleterious, with scores ranging from 29 to 34 (mean = 32)²⁹ (**Tab.1**). In addition, the *in-silico* classifiers MutPred2³⁰ and REVEL³¹ yielded scores that indicated high probabilities of pathogenicity for the variants (**Tab.1**). All four amino acids altered by the five nucleotide substitutions were phylogenetically conserved and found to lie within motifs that were invariant between different species, the four PMCA isoforms (except for Gly120 in ATP2B4), and all annotated ATP2B2 transcripts (**Fig.2A**). Furthermore, in support of a potential relevance to protein function, the variants were situated in regions depleted for nonsynonymous variation in the general population: bioinformatics calculations at base-pair-level resolution indicated that each alteration affected a site with significant intolerance to mutational lesions (as estimated by Wiel et al.³², variant at "intolerant" site, N=2; variant at "highly intolerant" site, N=2; **Fig.1C**). The recurrent p.(Gly120Arg)

variant localized to a segment between transmembrane domains 1 and 2 in the N-terminus, whereas the other variants mapped to the C-terminal third of the protein (cytosolic loop and transmembrane domains)⁵ (**Fig.1B/C**). Molecular modeling suggested that the variants may impact Ca^{2+} extrusion capacities of the pump either by interfering with Ca^{2+} binding or by perturbing other regulatory mechanisms (**Fig.2B**, **Suppl.Fig.1**). In more detail, c.3028G>A, p.(Glu1010Lys) and c.2633T>C, p.(Phe878Ser) affected the Ca^{2+} -binding region⁷, and replacement of Glu1010 by a lysine and Phe878 by a serine residue appeared to change local interactions with neighboring amino acids (charge substitution and loss of an aromatic side chain, respectively); Phe878 was located critically close to the Ca^{2+} -binding triad (Glu457, Asn914, and Asp918)⁷ and substitution with a serine would directly impact on ATP2B2's ability to bind Ca^{2+} (**Fig.2B**). The other amino acid substitutions identified were situated in structurally important motifs: c.2511G>T, p.(Met837Ile) was expected to potentially impact on phosphorylation of the catalytic aspartate⁷; moreover, c.358G>A and c.358G>C, both resulting in p.(Gly120Arg), were predicted to affect autoinhibitory interactions with the C-terminal segment³³ and/or the accessibility of the Ca^{2+} transport site by impairing the displacement of the calmodulin-binding autoinhibitory domain from the catalytic core³⁴. Both of these regulatory mechanisms would be disturbed by changes of residues around the transmembrane region 1 in the N-terminus. Two additional patients had *de novo* variants that were expected to be truncating: c.3338_3339del, p.(Val1113Glyfs*36) (individual 5) and c.3254dup, p.(Thr1086Aspfs*64) (individual 6) (**Tab.1**, **Fig.1A-C**, **Suppl.Fig.2**). Unlike nonsense, frameshift, and splicing variants detected in patients with isolated hearing loss¹³, these frameshifting alleles were located in the penultimate exon of *ATP2B2*, predicted to deleteriously affect the open reading frame that codes for the functional calmodulin-binding domain. Since localization of PTVs in the last or penultimate exon usually does

not lead to nonsense-mediated mRNA decay³⁵, the variants were likely to exert pathogenicity via a mechanism different from haploinsufficiency. In agreement with this hypothesis, *in-vitro* functional work has established that C-terminally truncated versions of PMCAs can give rise to specifically altered pump activities as a consequence of abolished interaction of calmodulin with the C-terminal regulatory regions²⁶. All seven identified *ATP2B2* variants, the missense and frameshift alterations, qualified as pathogenic alleles according to the ACMG classification standards (**Tab.1**)²⁵.

Clinical spectrum

The patient series consisted of three female and four male individuals ranging in age from 3 to 43 years (**Tab.1**). All patients were diagnosed with etiologically unexplained neurological or neurodevelopmental disorders with uninformative pre- and perinatal histories and no major congenital anomalies. Motor and/or language delay were present to a variable extent in the majority of individuals for whom this outcome could be evaluated (6/7). Intellectual disability of varying severity was documented in six individuals and all these subjects also had difficulties with verbal communication; absence of intelligible speech at the time of last assessment was noted for three patients. Other shared features common to most participants of the study were coordination and movement abnormalities (5/7) and epileptic signs (6/7). Five patients each had some degree of ataxic gait impairment ranging from minor imbalance to profound gait dysfunction; truncal and/or appendicular ataxia with other cerebellar signs such as intentional tremor and eye movement disorders were frequently observed. Variable expressions of epileptic phenotypes manifested within the first three years of life and included abnormal EEG findings without seizures (2/6) as well as focal myoclonic and generalized tonic-clonic seizures (4/6); two cases were

diagnosed with epileptic encephalopathy (individuals 5 and 6). Less consistent symptoms included behavioral disturbances (autism diagnosed in 3/6) and muscle tone alterations including hypotonia and dystonic posturing (3/6); a diagnosis of sensorineural hearing loss was established in only two of the patients (individuals 2 and 3 with *de novo* missense variants). A comparatively mild presentation, characterized by dystonic features, ataxia, and abnormal eye movements, was demonstrated by individual 1, whereas an unusually severe neurodevelopmental behavioral phenotype with marked autistic traits and rapid mood cycling was found in individual 3. Striking clinical overlap between unrelated subjects was registered in relation to variant recurrence and similar variant type: individuals 4 and 7 both harboring p.(Gly120Arg) shared almost identical manifestations of developmental delay, ataxia, muscular hypotonia, epilepsy, and cerebellar atrophy on brain MRI (**Fig.3**); moreover, for individuals 5 and 6 (each with a truncating variant), distinctive courses with progressive, difficult-to-control seizure activity and developmental stagnation were seen. Apart from MRI scans showing characteristic atrophic changes of the cerebellum in patients with the recurrent p.(Gly120Arg) variant (**Fig.3**), neuroimaging screenings were generally normal or considered nondiagnostic in the present series. Mild abnormal thinning of bilateral optic nerves on axial images was reported for individual 1 but the MRI was not available for review. Subtle and nonspecific facial dysmorphic aspects were noted in a few of the patients; for example, individuals 2 and 7 had epicanthic folds and a wide nasal bridge, among other variable individual signs. There were no consistent abnormalities described with respect to growth, vision, or other extraneural organ involvement. An overview about all assembled clinical data is given in **Tab.1**.

Expression studies and variant effects on Ca²⁺ transport function

The genetic and clinical data, especially the identification of *de novo* variants at sites under high codon selection in a severely variant-constrained gene and the genotype-specific similarities in phenotypic presentations provided strong evidence for pathogenicity of the collected variants. To test the variants' functionality and verify their potential harmful impact, we performed experiments in human cell culture (**Fig.4A-C**). Wild-type and mutant ATP2B2 expression constructs were generated and transfected into HeLa cells. In Western blot analyses, all mutant ATP2B2s demonstrated comparable levels to wild-type protein, with the exception of ATP2B2 harboring p.(Gly120Arg) which exhibited a marginally significant decrease in cellular abundance (**Fig.4A**). Overall, these findings were confirmed in immunocytochemistry stainings, demonstrating not only similar expression enrichment but also the proper localization at the plasma membrane for all mutants and the wild-type form (**Fig.4B**). Notably, the frameshift variant-containing pumps were also expressed without significant reduction of detected protein, consistent with the prediction that these variants will not trigger nonsense-mediated decay (**Fig.4A/B**). We then used an established co-transfection system with the Ca²⁺-sensing photoprotein aequorin to examine the impact of the patient variants on cytosolic Ca²⁺ concentration handling (**Fig.4C**). This method allows to assay activity of overexpressed PMCA pumps by determining the relative Ca²⁺ extrusion rate through analysis of [Ca²⁺]_{cyt} peaks after agonist-induced Ca²⁺ loading of the cytosol^{15,26}. We found that four variant-bearing versions of ATP2B2 including p.(Glu1010Lys), p.(Met837Ile), p.(Phe878Ser), and p.(Thr1086Aspfs*64) were associated with significantly elevated cytosolic Ca²⁺ peaks following histamine-induced Ca²⁺ transient increase as compared to the wild-type counterpart, compatible with compromised abilities of these mutant pumps to export Ca²⁺ to the extracellular environment (**Fig.4C**). The observed Ca²⁺ extrusion impairment was strongest for p.(Phe878Ser), carried by individual 3 with severe pediatric-onset neurodevelopmental

disease; ATP2B2 containing p.(Glu1010Lys), the variant identified in an adult patient with movement disorder and no major neurodevelopmental comorbidity (individual 1), exhibited only a moderate Ca²⁺ extrusion defect. By contrast, p.(Gly120Arg) and p.(Val1113Glyfs*36) resulted in gain-of-function effects with abnormally decreased stimulation-related Ca²⁺ peaks, indicative of ATP2B2 pump overactivity (**Fig.4C**). Collectively, the analyses indicated that all clinically observed variants caused significant changes in cytosolic Ca²⁺ handling under conditions of maximal cell stimulation, thus creating situations of intermittent intracellular Ca²⁺ dyshomeostasis.

Discussion

Unbiased sequencing-driven genetics studies and genotype-first approaches in the past few years have shown that different types of variants within the same gene and/or spatially diverse variant localizations in the gene product account for a substantial degree of heterogeneity in phenotypic outcomes^{16,36}. A handful of *ATP2B2* heterozygous PTVs with dominant inheritance or *de novo* transmission modes, mapping to the first two thirds of the encoded ATP2B2 pump, have recently been documented in families whose affected members manifested childhood-onset progressive hearing loss without accompanying neurological symptoms¹³. In addition, one adult patient with ataxia and intellectual disability carrying a missense variant of *ATP2B2* c.3427G>T, p.(Val1143Phe) has been published by our group before¹⁵. Although *in-vitro* experiments demonstrated decreased Ca²⁺ clearance from cells harboring the mutant construct¹⁵, evidence was still lacking to definitely link *ATP2B2* to ataxia and neurodevelopmental disorders. We now describe a group of individuals with heterozygous *ATP2B2* missense and end-truncating variants who expressed a distinct set of phenotypic abnormalities, further expanding the clinical spectrum of *ATP2B2*-related diseases to include developmental delay, speech impairment,

epilepsy, autism, and different types of movement and tone abnormalities. The observed features were compatible with phenotypic signs and symptoms described in association to variants in *ATP2B2*'s homologous genes *ATP2B1*¹⁰ and *ATP2B3*^{11,12}. In aggregate, the proven *de novo* status of most variants in our allelic series (6/7), the strong evolutionary conservation of altered amino acids, the overlapping phenotypes among the patients, our *in-silico* modeling data, and the experimentally confirmed impact of the variants on protein function supported the disease-causing nature of the *ATP2B2* alterations that we found. Consistent with this were also observations from rodent models, suggesting that *ATP2B2* plays an important role in brain development, neuronal Ca²⁺ homeostasis, and the control of voluntary movements³. Mouse mutants documenting a link between *Atp2b2* dysfunction and defective synaptic transmission in specific neural circuits have been reported for more than two decades^{3,4,7}, beginning with the description of “*deafwaddler*” mice displaying hearing impairment and early-onset ataxic phenotypes related to the spontaneous *Atp2b2* missense variant p.(Gly283Ser)³⁷; these animals have pronounced abnormalities in Purkinje cell morphology, indicative of cerebellar functional impairments³. Similarly, a second strain bearing the *Atp2b2* missense substitution p.(Glu412Lys), the “*wriggle mouse sagami*”, exhibits ataxic-like motility problems combined with dystonic involuntary limb posturing, most likely as a result of neuronal pathologies in the cerebellum³⁸. Cells from the *wriggle sagami* ataxic-dystonic mouse, in which dendritic spine development of Purkinje neurons is compromised, were shown to be characterized by increased basal cytosolic Ca²⁺ levels and impaired Ca²⁺ clearance following external stimulation³, reminiscent of what we saw in our functional studies with overexpressed mutant pumps. Furthermore, *Atp2b2* null and heterozygous knockout mice develop gene dosage loss-dependent ataxia resulting from functionally altered Purkinje-neuron Ca²⁺ signaling^{3,4,7}. Thus, the herein reported patients with *ATP2B2* variants manifested

phenotypic features highly similar to those observed in transgenic mice with *Atp2b2* pump defects, especially with regard to motor phenotypes (ataxia and/or dystonic features in 5/7 individuals), overt morphological changes of the cerebellum (cerebellar atrophy in individuals 4 and 7), and biochemical alterations in Ca^{2+} handling (Ca^{2+} extrusion dysfunction of mutant proteins in our *in-vitro* assays). Considering that the studies of ATP2B2 constructs engineered for four of the patients' variants including p.(Glu1010Lys), p.(Met837Ile), p.(Phe878Ser), and p.(Thr1086Aspfs*64) revealed diminished pump activities with increased peaks of cytosolic Ca^{2+} transients upon cell stimulation, the most likely possibility by which these variants might underlie disease is a partial (hypomorphic) loss-of-function effect. In our overexpression assay, two patient variants, namely p.(Gly120Arg) and p.(Val1113Glyfs*36), exhibited gain-of-function features, showing for the first time that hyperactivity of PMCA pumps can also be associated with disease. We observed molecular aberrations of varying severity in relation to specific variants and noted that, overall, the degree of functional alteration of the mutant pumps was comparatively modest in our cellular system with respect to the severe clinical syndromes presented by the majority of affected individuals in this study. The results were in good agreement with findings from functional evaluations of Ca^{2+} handling defects in other PMCA-linked conditions such as *ATP2B3*-associated ataxia²⁶; it has been highlighted that the absolute contribution of PMCA to Ca^{2+} clearance is rather minor compared to other existing cellular Ca^{2+} transport systems, but individual PMCA perturbation may have significant impact on fine regulation of Ca^{2+} homeostasis in certain brain micro-circuits and neuronal sub-domains^{7,8}. For the two truncating variants, a plausible mechanism of pathogenicity is a protein function-altering effect arising as a consequence of disturbance of the calmodulin-binding C-terminal regulatory domain and its interplay with the autoinhibitory site in the N-terminus of the protein. Previous work has shown that targeted ablation and missense

variants of the calmodulin-binding region result in the inability of PMCAs to properly control cytosolic Ca^{2+} .^{6,26} Intriguingly, the truncating variants seen in our patients affected protein function in distinct ways, variant p.(Thr1086Aspfs*64) in a loss-of-function and the other one p.(Val1113Glyfs*36) in a gain-of-function direction. Although currently speculative, the opposite effects may be derived from the differing nature of the neopeptides generated by the frameshifts, i.e., p.(Thr1086Aspfs*64) versus p.(Val1113Glyfs*36) (**Suppl.Fig.2**), which may lead to different (residual) abilities of the mutant ATP2B2s to bind calmodulin. The pathogenic molecular effects of our frameshift variants are likely to be different from those induced by haploinsufficient PTV alleles found in patients affected with isolated hearing loss¹³. We point out, however, that the two additional *ATP2B2* *de novo* PTVs c.2268C>A, p.(Cys756*) and c.3191G>A, p.(Trp1064*), one of which was located in the vicinity of the variant c.2329C>T, p.(Arg777*) associated with hearing loss from Smits et al.¹³ (**Fig.1C**), were prioritized as top disease-causal candidates in a large cohort of patients with autism spectrum disorders (no further phenotypic details available)³⁹. Therefore, it is possible that *ATP2B2* haploinsufficiency might also be at play in neurodevelopmental diseases and that a phenotypical continuum exists, ranging from apparently non-syndromic hearing impairment at the mild end to autistic traits and potential other features at the more severe end. The phenotypes presented by the patients in our series establish a wide spectrum of neurological-disease features associated with genetic variation at *ATP2B2*. Based on the clinical observations that we made, some preliminary genotype-phenotype correlations may emerge, although certainly additional studies will be required to confirm these findings. First, we saw notable similarities in phenotypic abnormalities among individuals with recurrent variation at codon 120; these phenotypes appeared rather distinct and comprised mainly prominent muscular hypotonia, ataxia, cerebellar atrophy, and epilepsy. Moreover, there were differences

in disease manifestations between individuals with missense substitutions and those with C-terminal frameshift variants (more severe developmental and epileptic morbidity in the latter group). Second, we noted some degree of correlation between clinical severity and the biochemical alterations at the cellular level: the Ca²⁺ extrusion dysfunction was not dramatic, although significant as compared to wild-type, for a variant carried by a mildly affected adult patient (individual 1), while the aberrations were more pronounced for some other variants found in pediatric neurodevelopmental-disorder cases. Although we could functionally characterize all herein identified mutant ATP2B2 pumps based on their decreased or enhanced abilities to clear cytosolic Ca²⁺ transients, our cellular assay was likely to be unable to capture all molecular phenotypic outcomes in a human physiological context. Brain (or particular brain subregion)-specific consequences of individual *ATP2B2* pathogenic variants are hard to define, and therefore it remains difficult to determine why there was no clear relationship between the severity of symptoms and the observed impact of variants on Ca²⁺ handling when comparing individual 1 (mild adult phenotype) and individual 2 (pronounced neurodevelopmental phenotype). Moreover, we found no obvious group differences in phenotypes between individuals heterozygous for *ATP2B2* loss-of-function variants (N=4) and those with heterozygous gain-of-function variants (N=3); rather, the two patients with frameshift variants, of which one was experimentally classified as a loss-of-function (individual 6) and one as a gain-of-function (individual 5) allele, appeared to be more phenotypically similar to each other than some other cases within the loss-or gain-of-function groups. Identification of further independent patients and future in-depth functional evaluations may help to better understand genotype-to-phenotype relationships in *ATP2B2*-related disorders. Taken together, our data reinforce the concept that Ca²⁺ dyshomeostasis represents a major driver of neurocognitive, epileptic, and movement disorders under the background of abnormal

neurodevelopment¹. Our understanding of the biological mechanisms that allow cells to dynamically respond to the changing needs of Ca^{2+} signaling and the associated pathophysiological implications are only beginning to emerge and essentially depend on insights from human disease studies⁸. We here demonstrate that *de novo* missense and specific truncating variants in one of the four major ATP-dependent plasma membrane Ca^{2+} pumps, *ATP2B2*, cause movement and neurodevelopmental disorders. We propose that the phenotypes result from defects in the tight control of intracellular Ca^{2+} concentrations and that the localization and individual functional consequences of *ATP2B2* variants may contribute to variability in presentations and disease severity. Future work should address the precise effects of different *ATP2B2* variant types in brain micro-circuitry and explore the potential of *ATP2B2* as a therapeutic target.

Data Availability

All data and materials that are not included in the paper are available upon request.

Acknowledgements

We are grateful to the patients and their families for their participation. MZ is a member of the Medical and Scientific Advisory Council of the Dystonia Medical Research Foundation.

Funding Statement

This study was funded in part by a research grant from the Else Kröner-Fresenius-Stiftung, as well as by in-house institutional funding from Technische Universität München, Munich, Germany, Helmholtz Zentrum München, Munich, Germany, and

research support from the German Research Foundation awarded to JW and MZ (DFG 458949627; WI 1820/14-1; ZE 1213/2-1). MZ acknowledges grant support by the EJP RD, the European Joint Programme on Rare Diseases (EJP RD Joint Transnational Call 2022), and the German Federal Ministry of Education and Research (BMBF, Bonn, Germany), awarded to the project PreDYT (PREdictive biomarkers in DYsTonia, 01GM2302), by the Federal Ministry of Education and Research (BMBF) and the Free State of Bavaria under the Excellence Strategy of the Federal Government and the Länder, as well as by the Technical University of Munich – Institute for Advanced Study. RK and HP acknowledge grant support from the German Federal Ministry of Education and Research (BMBF, Bonn, Germany) awarded to the German Network for Mitochondrial Disorders (mitoNET, 01GM1906A). The work was also supported by the National Institute for Neurological Research, Czech Republic, Programme EXCELES, ID Project No. LX22NPO5107, funded by the European Union – Next Generation EU and also by the Charles University: Cooperatio Program in Neuroscience. The work was further supported by grants from the Ministry of University and Research (Bando SIR 2014 no. RBSI14C65Z and PRIN2017 to T.C.) and from the Università degli Studi di Padova (Progetto Giovani 2012 no. GRIC128SP0 to T.C., Progetto di Ateneo 2016 no. CALI_SID16_01 to T.C., STARS Consolidator Grant 2019 to T.C. and Progetto di Ateneo 2015 no. CPDA153402 to M.B.). Natalia Julia-Palacios is supported by FIS P118/00111 and FI21/0073 “Instituto de Salud Carlos III (ISCIII)” and “Fondo Europeo de desarrollo regional (FEDER). This work was supported in part by Telethon Undiagnosed Diseases Program (TUDP, GSP15001).

Author Contributions

Conceptualization: T.C., M.B., M.Z.; Data Curation: A.G.C., S.S.J., N.J.-P., B.K., R.K., S.A.L., C.M., C.Mor., C.N., V.N., A.O., H.P., V.S., N.S., A.T., P.V., E.Y., M.Zol., R.J.,

J.W., J.N.; Formal analysis: E.P., L.B., A.S., C.M., A.D., T.C., M.B., M.Z.; Writing-original draft: T.C., M.B., M.Z.; Writing-review and editing: all authors.

Ethics Declaration

Individuals were identified in different centers worldwide in diagnostic or research settings approved by the respective institutional review boards. All affected individuals or their legal representatives gave informed consent for the sequencing procedures and the publication of their results along with clinical and molecular data. Data was de-identified. This study adhered to the World Medical Association Declaration of Helsinki (2013). Permission was obtained to publish patient MR images. The study was performed within the framework of a gene discovery initiative for rare diseases which has ethical approval from the appropriate review board of Technical University of Munich.

Conflict of Interest

The authors declare that they have no competing financial and/or non-financial interests related to this study.

References

1. Kawamoto EM, Vivar C, Camandola S. Physiology and pathology of calcium signaling in the brain. *Front Pharmacol.* 2012;3:61.
2. Brini M, Ottolini D, Cali T, Carafoli E. Calcium in health and disease. *Met Ions Life Sci.* 2013;13:81-137.

3. Stafford N, Wilson C, Oceandy D, Neyses L, Cartwright EJ. The Plasma Membrane Calcium ATPases and Their Role as Major New Players in Human Disease. *Physiol Rev.* 2017;97(3):1089-1125.
4. Krebs J. Structure, Function and Regulation of the Plasma Membrane Calcium Pump in Health and Disease. *Int J Mol Sci.* 2022;23(3).
5. Brini M. Plasma membrane Ca(2+)-ATPase: from a housekeeping function to a versatile signaling role. *Pflugers Arch.* 2009;457(3):657-664.
6. Cali T, Frizzarin M, Luoni L, et al. The ataxia related G1107D mutation of the plasma membrane Ca(2+) ATPase isoform 3 affects its interplay with calmodulin and the autoinhibition process. *Biochim Biophys Acta Mol Basis Dis.* 2017;1863(1):165-173.
7. Brini M, Cali T, Ottolini D, Carafoli E. The plasma membrane calcium pump in health and disease. *FEBS J.* 2013;280(21):5385-5397.
8. Cali T, Brini M, Carafoli E. The PMCA pumps in genetically determined neuronal pathologies. *Neurosci Lett.* 2018;663:2-11.
9. Hamosh A, Scott AF, Amberger JS, Bocchini CA, McKusick VA. Online Mendelian Inheritance in Man (OMIM), a knowledgebase of human genes and genetic disorders. *Nucleic Acids Res.* 2005;33(Database issue):D514-517.
10. Rahimi MJ, Urban N, Wegler M, et al. De novo variants in ATP2B1 lead to neurodevelopmental delay. *Am J Hum Genet.* 2022;109(5):944-952.
11. Cali T, Lopreiato R, Shimony J, et al. A Novel Mutation in Isoform 3 of the Plasma Membrane Ca²⁺ Pump Impairs Cellular Ca²⁺ Homeostasis in a Patient with Cerebellar Ataxia and Laminin Subunit 1alpha Mutations. *J Biol Chem.* 2015;290(26):16132-16141.
12. Feyma T, Ramsey K, Group CRR, et al. Dystonia in ATP2B3-associated X-linked spinocerebellar ataxia. *Mov Disord.* 2016;31(11):1752-1753.

13. Smits JJ, Oostrik J, Beynon AJ, et al. De novo and inherited loss-of-function variants of ATP2B2 are associated with rapidly progressive hearing impairment. *Hum Genet.* 2019;138(1):61-72.
14. Karczewski KJ, Francioli LC, Tiao G, et al. The mutational constraint spectrum quantified from variation in 141,456 humans. *Nature.* 2020;581(7809):434-443.
15. Vicario M, Zanni G, Vallese F, et al. A V1143F mutation in the neuronal-enriched isoform 2 of the PMCA pump is linked with ataxia. *Neurobiol Dis.* 2018;115:157-166.
16. Sobreira N, Schiettecatte F, Valle D, Hamosh A. GeneMatcher: a matching tool for connecting investigators with an interest in the same gene. *Hum Mutat.* 2015;36(10):928-930.
17. Zech M, Jech R, Boesch S, et al. Monogenic variants in dystonia: an exome-wide sequencing study. *Lancet Neurol.* 2020;19(11):908-918.
18. Rosenhahn E, O'Brien TJ, Zaki MS, et al. Bi-allelic loss-of-function variants in PPFIBP1 cause a neurodevelopmental disorder with microcephaly, epilepsy, and periventricular calcifications. *Am J Hum Genet.* 2022;109(8):1421-1435.
19. Dias KR, Carlston CM, Blok LER, et al. De Novo ZMYND8 variants result in an autosomal dominant neurodevelopmental disorder with cardiac malformations. *Genet Med.* 2022;24(9):1952-1966.
20. Adamo CS, Beyens A, Schiavinato A, et al. EMILIN1 deficiency causes arterial tortuosity with osteopenia and connects impaired elastogenesis with defective collagen fibrillogenesis. *Am J Hum Genet.* 2022;109(12):2230-2252.
21. Kim SY, Jang SS, Kim H, et al. Genetic diagnosis of infantile-onset epilepsy in the clinic: Application of whole-exome sequencing following epilepsy gene panel testing. *Clin Genet.* 2021;99(3):418-424.

22. Al-Jawahiri R, Foroutan A, Kerkhof J, et al. SOX11 variants cause a neurodevelopmental disorder with infrequent ocular malformations and hypogonadotropic hypogonadism and with distinct DNA methylation profile. *Genet Med.* 2022;24(6):1261-1273.
23. Zech M, Kopajtich R, Steinbrucker K, et al. Variants in Mitochondrial ATP Synthase Cause Variable Neurologic Phenotypes. *Ann Neurol.* 2022;91(2):225-237.
24. Dzinovic I, Boesch S, Skorvanek M, et al. Genetic overlap between dystonia and other neurologic disorders: A study of 1,100 exomes. *Parkinsonism Relat Disord.* 2022;102:1-6.
25. Richards S, Aziz N, Bale S, et al. Standards and guidelines for the interpretation of sequence variants: a joint consensus recommendation of the American College of Medical Genetics and Genomics and the Association for Molecular Pathology. *Genet Med.* 2015;17(5):405-424.
26. Zanni G, Cali T, Kalscheuer VM, et al. Mutation of plasma membrane Ca²⁺ ATPase isoform 3 in a family with X-linked congenital cerebellar ataxia impairs Ca²⁺ homeostasis. *Proc Natl Acad Sci U S A.* 2012;109(36):14514-14519.
27. Brini M, Marsault R, Bastianutto C, Alvarez J, Pozzan T, Rizzuto R. Transfected aequorin in the measurement of cytosolic Ca²⁺ concentration ([Ca²⁺]_c). A critical evaluation. *J Biol Chem.* 1995;270(17):9896-9903.
28. Rizzuto R, Brini M, Bastianutto C, Marsault R, Pozzan T. Photoprotein-mediated measurement of calcium ion concentration in mitochondria of living cells. *Methods Enzymol.* 1995;260:417-428.
29. Kircher M, Witten DM, Jain P, O'Roak BJ, Cooper GM, Shendure J. A general framework for estimating the relative pathogenicity of human genetic variants. *Nat Genet.* 2014;46(3):310-315.

30. Pejaver V, Urresti J, Lugo-Martinez J, et al. Inferring the molecular and phenotypic impact of amino acid variants with MutPred2. *Nat Commun.* 2020;11(1):5918.
31. Ioannidis NM, Rothstein JH, Pejaver V, et al. REVEL: An Ensemble Method for Predicting the Pathogenicity of Rare Missense Variants. *Am J Hum Genet.* 2016;99(4):877-885.
32. Wiel L, Baakman C, Gilissen D, Veltman JA, Vriend G, Gilissen C. MetaDome: Pathogenicity analysis of genetic variants through aggregation of homologous human protein domains. *Hum Mutat.* 2019;40(8):1030-1038.
33. Mazzitelli LR, Adamo HP. Hyperactivation of the human plasma membrane Ca²⁺ pump PMCA h4xb by mutation of Glu99 to Lys. *J Biol Chem.* 2014;289(15):10761-10768.
34. Bredeston LM, Adamo HP. Loss of autoinhibition of the plasma membrane Ca(2+) pump by substitution of aspartic 170 by asparagin. A ctivation of plasma membrane calcium ATPase 4 without disruption of the interaction between the catalytic core and the C-terminal regulatory domain. *J Biol Chem.* 2004;279(40):41619-41625.
35. Popp MW, Maquat LE. Leveraging Rules of Nonsense-Mediated mRNA Decay for Genome Engineering and Personalized Medicine. *Cell.* 2016;165(6):1319-1322.
36. Harel T, Yesil G, Bayram Y, et al. Monoallelic and Biallelic Variants in EMC1 Identified in Individuals with Global Developmental Delay, Hypotonia, Scoliosis, and Cerebellar Atrophy. *Am J Hum Genet.* 2016;98(3):562-570.
37. Street VA, McKee-Johnson JW, Fonseca RC, Tempel BL, Noben-Trauth K. Mutations in a plasma membrane Ca²⁺-ATPase gene cause deafness in deafwaddler mice. *Nat Genet.* 1998;19(4):390-394.

38. Inoue Y, Matsumura Y, Inoue K, Ichikawa R, Takayama C. Abnormal synaptic architecture in the cerebellar cortex of a new dystonic mutant mouse, Wriggle Mouse Sagami. *Neurosci Res.* 1993;16(1):39-48.
39. Takata A, Miyake N, Tsurusaki Y, et al. Integrative Analyses of De Novo Mutations Provide Deeper Biological Insights into Autism Spectrum Disorder. *Cell Rep.* 2018;22(3):734-747.
40. Omasits U, Ahrens CH, Muller S, Wollscheid B. Protter: interactive protein feature visualization and integration with experimental proteomic data. *Bioinformatics.* 2014;30(6):884-886.

Figure legends

Figure 1 Heterozygous *ATP2B2* variants in seven individuals and their respective locations on ATP2B2 protein

(A) Simplified pedigrees for individuals 1-7 with detected variants in *ATP2B2*. Black circles and squares represent affected female and male patients, respectively. Open symbols represent unaffected parents. Trio whole-exome sequencing was carried out in families of individuals 1-6. DNA from the healthy father of individual 7 was not available for genetic testing (N/A). Identified genotypes at the *ATP2B2* locus, including four missense changes (one recurrent variation at amino acid position Gly120) and two frameshift variants, are indicated below the individuals' family trees; a *de novo* status was proven for six out of the seven patient variants. (B) Topological illustration of the *ATP2B2*-encoded protein ATP2B2 (GenBank: NM_001001331; Uniprot: Q01814) depicting ten transmembrane domains (numbered), two cytosolic loop domains, and a C-terminal intracellular tail containing the calmodulin-binding regulatory domain. Black represents missense variants and red represents truncating (frameshift) variants. The Protter online tool (<https://wlab.ethz.ch/protter/start/>)⁴⁰ was used for ATP2B2 protein

visualization. (C) Representation of the variant tolerance landscape of ATP2B2 and distribution of variants identified in patients. All amino acid residues affected by missense variants are intolerant to functional genetic variation according to the MetaDome web server (<https://stuart.radboudumc.nl/metadome/>)³². A schematic of ATP2B2 is indicated underneath the MetaDome plot, along with the truncating variants identified in patients. The missense variants in black and the frameshift variants in red were detected in individuals with movement and neurodevelopmental disorders in the present work. The missense variant in gray has been reported previously in a patient with ataxia¹⁵; the truncating variants in blue and purple have been described in subjects with isolated hearing loss¹³ and autism/neurodevelopmental disease³⁹, respectively. Note the most C-terminal localization of truncating variants identified in this study.

Figure 2 *ATP2B2* missense variant conservation and modeling

(A) Multiple amino-acid sequence alignments showing an extremely high degree of conservation of all residues affected by missense variants identified in this study. A multi-species alignment (upper panel) as well as alignments between sequences of the four different plasma membrane Ca^{2+} ATPase isoforms (ATP2B1-4, encoded by *ATP2B1-ATP2B4*; middle panel) and all ATP2B2 transcript variants (lower panel) are illustrated. Uniprot identifiers of the transcripts are provided. (B) 3D structural analysis of herein identified missense variants using a ribbon presentation of the ATP2B2 pump in the Ca^{2+} -free state. Upper panel: the relative positions of variants are highlighted in red on an overview (left) and on magnified views (right) of ATP2B2; magnifications are indicated by dashed white lines. The variants p.(Phe878Ser) and p.(Glu1010Lys) are located in the Ca^{2+} -binding region, whereas the p.(Met837Ile) substitution affects a residue with potential involvement in activity-dependent conformational changes of the pump and the associated phosphorylation of the catalytic aspartate residue (D499,

yellow arrow). The recurrent p.(Gly120Arg) variant falls into the N-terminal part of the protein which contains integral elements required for activity regulation of the pump. Lower panel: model of the Ca²⁺-binding region with the critical amino acid residues Glu457, Asn914, and Asp918 (yellow) essentially involved in Ca²⁺ binding and the site of the p.(Phe878Ser) variant (red). Loss of the phenylalanine aromatic side chain (F878) would critically alter local bonding interactions with the Ca²⁺-binding triad (Glu457-Asn914-Asp918, in yellow), likely leading to an impaired ability of ATP2B2 to bind Ca²⁺ with severe functional perturbation. Additional results of *in silico* modeling for the mutant ATP2B2 pumps can be found in Suppl. Fig. 1.

Figure 3 Magnetic resonance imaging results for patients with the recurrent p.(Gly120Arg) substitution associated with cerebellar morphological changes

T2 FLAIR-weighted (a) and T1-weighted (b-d) sagittal brain MRI scans of individual 4 carrying *ATP2B2* c.358G>A, p.(Gly120Arg) at the ages of 5 months (a), 1 year and 5 months (b), 2 years and 1 month (c), and 3 years and 1 month (d). Note progressive atrophy of the cerebellum. (e-h) Brain MRI scans of individual 7 carrying *ATP2B2* c.358G>C, p.(Gly120Arg) at the age of 8 years. Cerebellar atrophic abnormalities are depicted in sagittal T2-FLAIR (e), axial fast spin-echo (f), sagittal T2 CUBE (g), and coronal T2-FLAIR (h) sequences.

Figure 4 Functional evaluation of *ATP2B2* variants found in the present cohort of previously unreported individuals

(A and B) Wild-type (WT) and mutant human ATP2B2 constructs (hPMCA2b) were transfected into HeLa cells and PMCA expression was assessed by Western blot (A) and immunocytochemistry (B) analyses. Control (CTR) cells were transfected with empty vector. The monoclonal mouse antibody 5F10 was used for PMCA detection.

The variants p.(Thr1086Aspfs*64) (individual 6), p.(Gly120Arg) (individuals 4 and 7), p.(Val1113Glyfs*36) (individual 5), p.(Met837Ile) (individual 2), p.(Glu1010Lys) (individual 1), and p.(Phe878Ser) (individual 3) are indicated by T1086fs, G120R, V1113fs, M837I, E1010K, and F878S, respectively. (A) Representative immunoblots using 5F10 and anti-actin (loading control) antibodies are shown. Results from densitometric quantifications of the levels of overexpressed ATP2B2s referred to actin are provided in the underneath panel. Data are expressed as mean \pm SD from 5 independent experiments. ns, not significant; *, $p < 0.05$; **, $p < 0.01$. (B) Representative immunocytochemical stainings showing the expression level and cellular localization of the wild-type (WT) and mutant ATP2B2. Note unaltered expression and normal distribution of the frameshift variant-bearing pumps (T1086fs and V1113fs). Scale bars indicate 20 μ m. (C) Ca²⁺ measurements in HeLa cells transiently overexpressing wild-type (WT) or mutant ATP2B2 pumps. The patient-derived variants are indicated as in (A) and (B). Cytosolic Ca²⁺ transients were recorded following histamine stimulation of cells co-transfected with the aequorin construct (cytAEQ) and the empty vector (CTR) or ATP2B2-expressing plasmids. Left panel: the curves represent the average of the single traces considered for the quantification analysis on the values of [Ca²⁺]_{cyt} peaks shown in the right panel. Right panel: average peak [Ca²⁺]_{cyt} values measured upon stimulation (bars represent mean μ M \pm SEM). The numbers of the dots indicate the number of independent measurements out of four independent transfections. Specific sample sizes analyzed were as follows: CTR, n=70; WT, n=72; M837I, n=65; E1010K, n=55; G120R, n=30; V1113fs, n=35; T1086fs, n=36; F878S, n=62. **, $p < 0.01$; ****, $p < 0.0001$; ns, not significant.

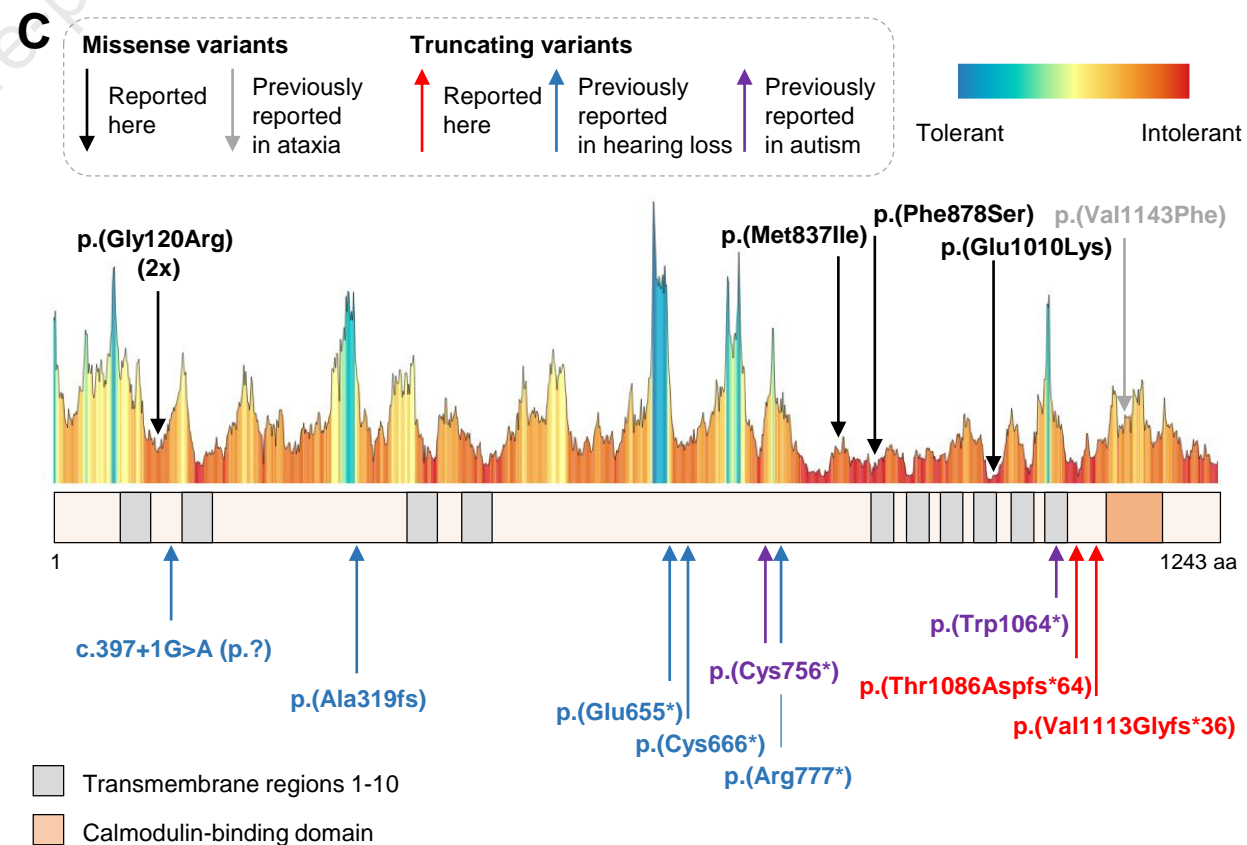
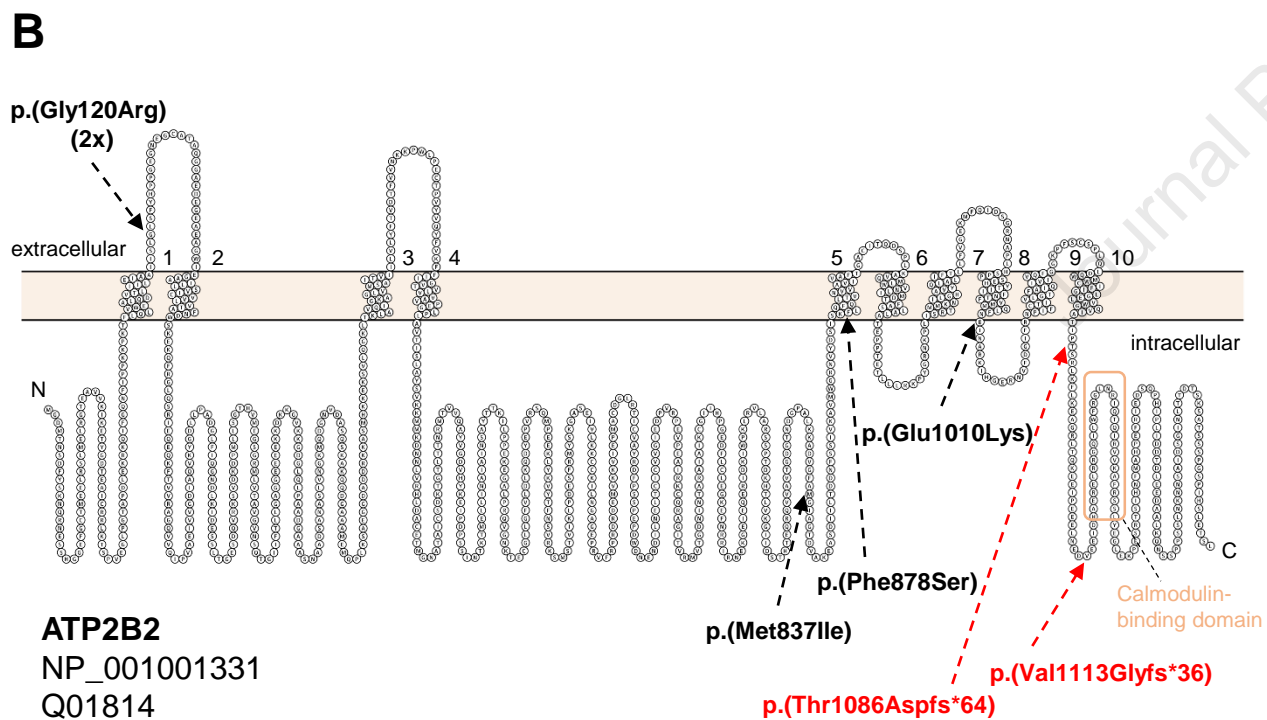
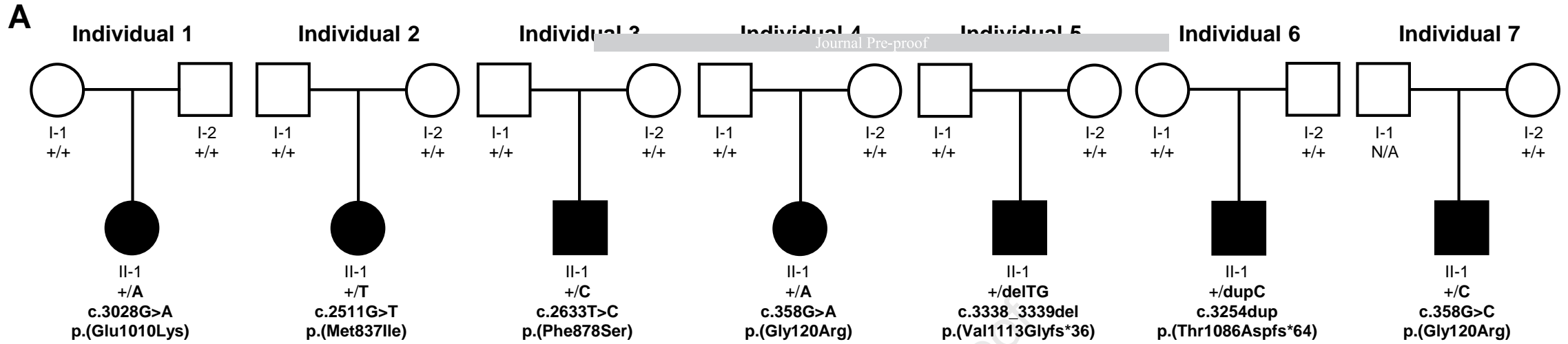
Table 1 List of molecular and phenotypic features of seven individuals with heterozygous *ATP2B2* variants

	Individual 1	Individual 2	Individual 3	Individual 4	Individual 5	Individual 6	Individual 7	Summary
<i>ATP2B2</i> variant RefSeq transcript: NM_001001331.4	c.3028G>A, p.(Glu1010Lys)	c.2511G>T, p.(Met837Ile)	c.2633T>C, p.(Phe878Ser)	c.358G>A, p.(Gly120Arg)	c.3338_3339del, p.(Val1113Glyfs*36)	c.3254dup, p.(Thr1086Aspfs*64)	c.358G>C, p.(Gly120Arg)	missense SNVs: 5/7; frameshift indels: 2/7
Family structure	trio	trio	trio	trio	trio	trio	mother-patient	trio: 6/7
Inheritance	<i>de novo</i>	<i>de novo</i>	<i>de novo</i>	<i>de novo</i>	<i>de novo</i>	<i>de novo</i>	non-maternal (father not available)	confirmed <i>de novo</i> : 6/7
Allele frequency (gnomAD v2.1 and v3.1/ >30,000 in-house control exomes)	not found	not found	not found	not found	not found	not found	not found	absent from controls: 7/7
CADD score	34	33	29.2	33	N/A	N/A	32	29.2 – 34 (5 missense SNVs)
MutPred2 rank score	0.911	0.935	0.932	0.931	N/A	N/A	0.931	0.911 – 0.935 (5 missense SNVs)
REVEL rank score	0.995	0.993	0.995	0.975	N/A	N/A	0.975	0.975 – 0.995 (5 missense SNVs)
ACMG classification (applied criteria)	pathogenic (PS2, PS3, PM1, PM2, PP2, PP3)	pathogenic (PS2, PS3, PM1, PM2, PP2, PP3)	pathogenic (PS2, PS3, PM1, PM2, PP2, PP3)	pathogenic (PS2, PS3, PM1, PM2, PP2, PP3)	pathogenic (PS2, PS3, PM2)	pathogenic (PS2, PS3, PM2)	pathogenic (PS1, PS3, PM1, PM2, PP2, PP3)	pathogenic: 7/7
Other candidate variants	no	no	no	no	no	no	no	no alternative genetic diagnoses: 7/7
Sex	female	female	male	female	male	male	male	female: 3/7; male: 4/7
Age	43 years	10 years	14 years	3 years	6 years	7.5 years	14 years	3 – 43 years
Ancestry	European	European	European/ Asian	European	Asian	European	European	European: 5/7; Asian: 1/7; mixed: 1/7
Clinical diagnosis	ataxia-dystonia syndrome	NDD	NDD (predominant behavioral deficits)	NDD/ congenital ataxia	NDD/ epileptic encephalopathy	NDD/ epileptic encephalopathy	congenital ataxia	ataxia syndrome: 3/7; NDD: 5/7
Global developmental delays	ND	+++	++	++	++	++	+++	6/7
Intellectual disability	-	+++	++	+++	++	++	+++	6/7
Behavioral deficits	-	+, aggressive	+++; autism	++ ^a	-	++, autism	++, autism	5/7
Speech impaired	-	+	++	+++; absent speech	+++; absent speech	++	+++; absent speech	6/7
Motor impaired	+	+	-	+++	+	-	+	5/7
Ataxia	+++	++	-	+++	++	-	+++	5/7
Muscle tone abnormalities/ movement disorders	+, dystonic signs ^b	-	-	+++; hypo	-	-	++, hypo	3/7
Seizures/EEG abnormalities	-	+, abnormal EEG	+, abnormal EEG	++, myoclonic seizures	+++; epileptic encephalopathy	+++; epileptic encephalopathy	++, generalized tonic-clonic seizures	6/7
Dysmorphic features	-	+	-	-	-	-	+	2/7
Hearing abnormalities	-	+, hearing loss	+, hearing loss	NR	-	NR	NR	2/7
Ophthalmological abnormalities	+, optic atrophy	-	-	+, strabismus	+, strabismus	NR	+, oculomotor apraxia	4/7

Brain MRI abnormalities	-	-	-	+, cerebellar atrophy (progressive)	-	-	+, cerebellar atrophy	2/7
-------------------------	---	---	---	-------------------------------------	---	---	-----------------------	-----

ACMG, American College of Medical Genetics and Genomics; CADD, combined annotation dependent depletion; EEG, electroencephalography; hypo, muscular hypotonia; MRI, magnetic resonance imaging; N/A, not available; ND, no data; NDD, neurodevelopmental disorder; NR, not reported; REVEL, rare exome variant ensemble learner; ^a autistic-like behaviors were observed, but autism was not formally diagnosed. ^b good response to botulinum toxin injection therapy. +/+/+++ symbols indicate the degree to which the feature(s) was (were) present.

Journal Pre-proof



A

Different species

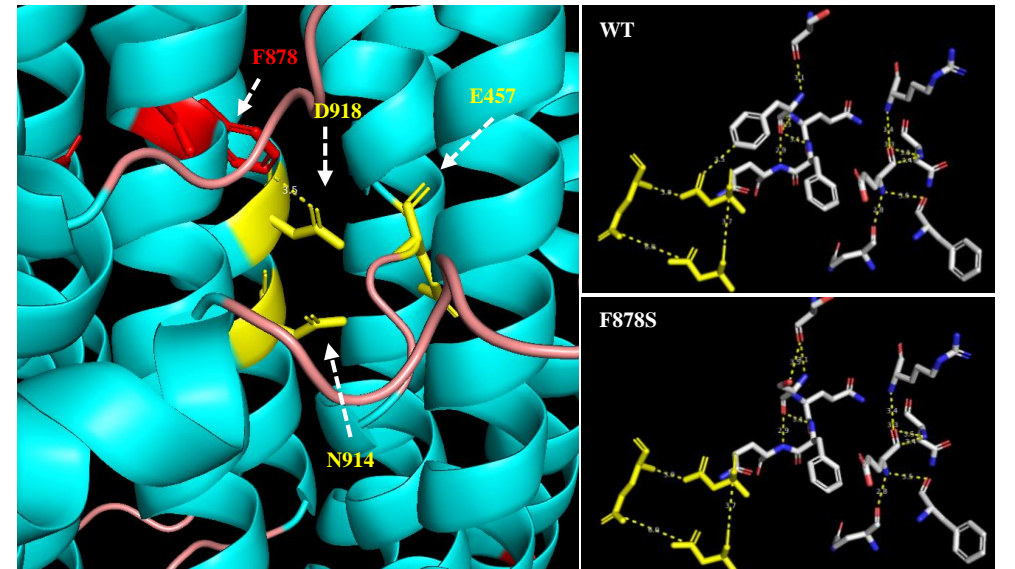
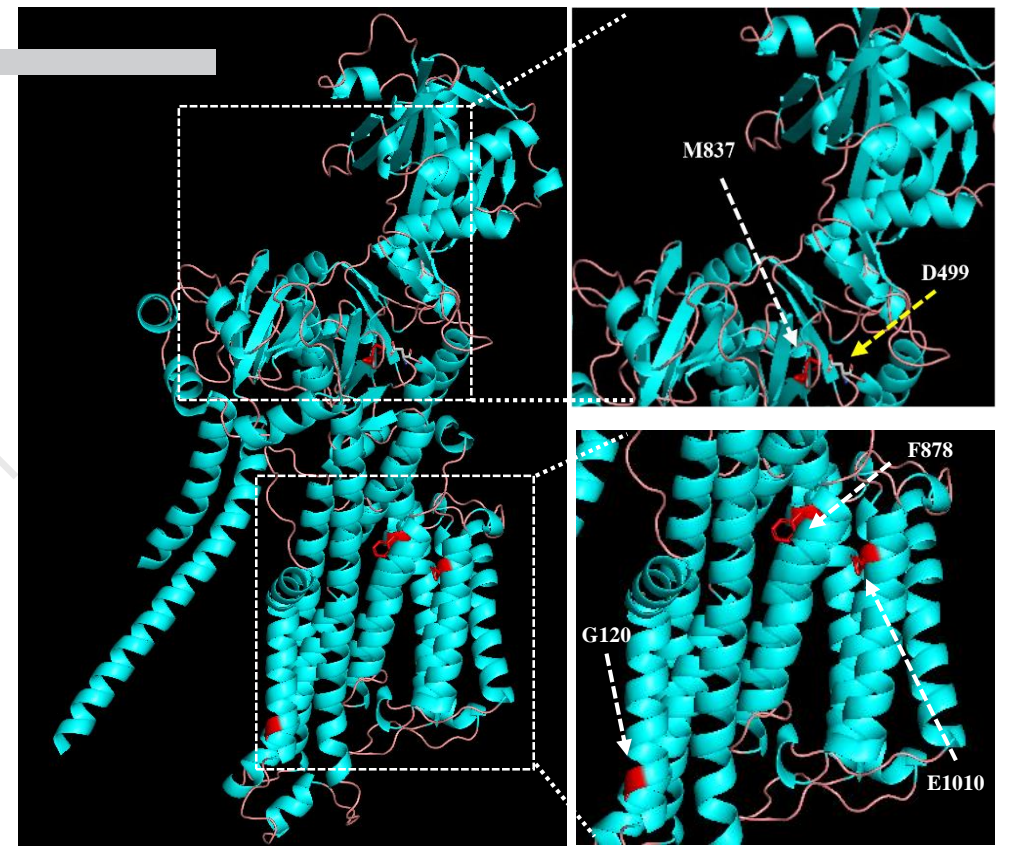
	G120	M837	F878	E1010
Xenopus tropicalis	ILEIAAIIISLGSFYRPPGG	ALKKADVGFAMGIAGTDVAKE	RNVYDSISKFLQFQLTNVN	TFVMMQLFNEINARKIHGERI
Danio rerio	ILEIAAIIISLGSFYQPPGG	ALKKADVGFAMGIAGTDVAKE	RNVYDSISKFLQFQLTNVN	TFVMMQLFNEINARKIHGERI
Mus musculus	ILEIAAIIISLGSFYHPPGG	ALKKADVGFAMGIAGTDVAKE	RNVYDSISKFLQFQLTNVN	TFVMMQLFNEINARKIHGERI
Homo sapiens	ILEIAAIIISLGSFYHPPGG	ALKKADVGFAMGIAGTDVAKE	RNVYDSISKFLQFQLTNVN	TFVMMQLFNEINARKIHGERI
Rattus norvegicus	ILEIAAIIISLGSFYHPPGG	ALKKADVGFAMGIAGTDVAKE	RNVYDSISKFLQFQLTNVN	TFVMMQLFNEINARKIHGERI

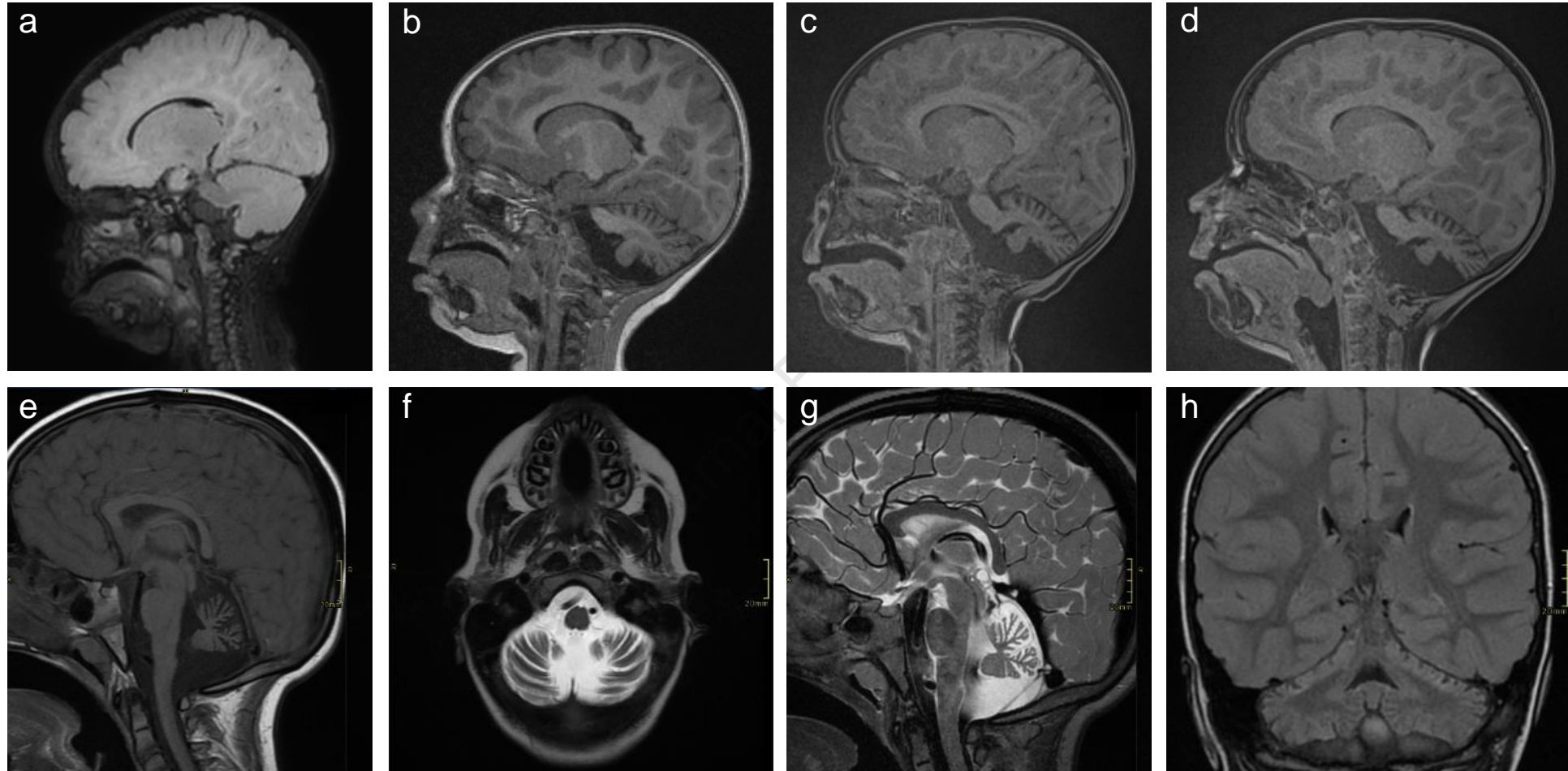
PMCA isoforms

	G120	M837	F878	E1010
AT2B1_HUMAN	AIVSLGLLSF	VGFAMGIAG	ISKFLQFQ	LFNEINARK
AT2B2_HUMAN	AIVSLGLLSF	VGFAMGIAG	ISKFLQFQ	LFNEINARK
AT2B3_HUMAN	AIVSLGLLSF	VGFAMGIAG	ISKFLQFQ	LFNEINARK
AT2B4_HUMAN	AIVSLVLSF	VGFAMGIAG	ISKFLQFQ	LFNEINSRK

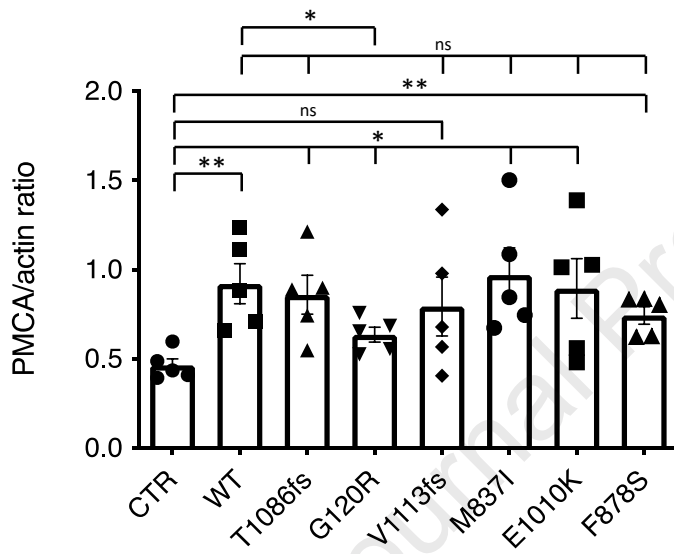
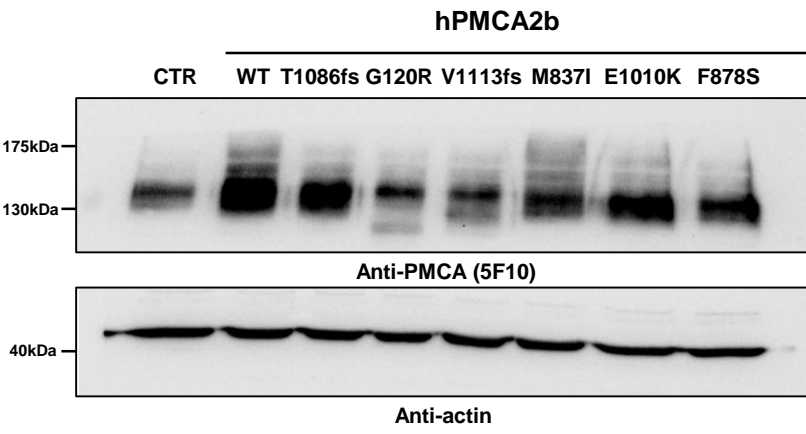
ATP2B2 transcript variants

	G120	M837	F878	E1010
Q01814-1 / AT2B2_HUMAN	AIVSLGLLSF	VGFAMGIAG	ISKFLQFQ	LFNEINARK
Q01814-2 / AT2B2_HUMAN	AIVSLGLLSF	VGFAMGIAG	ISKFLQFQ	LFNEINARK
Q01814-3 / AT2B2_HUMAN	AIVSLGLLSF	VGFAMGIAG	ISKFLQFQ	LFNEINARK
Q01814-4 / AT2B2_HUMAN	AIVSLGLLSF	VGFAMGIAG	ISKFLQFQ	LFNEINARK
Q01814-5 / AT2B2_HUMAN	AIVSLGLLSF	VGFAMGIAG	ISKFLQFQ	LFNEINARK
Q01814-6 / AT2B2_HUMAN	AIVSLGLLSF	VGFAMGIAG	ISKFLQFQ	LFNEINARK
Q01814-7 / AT2B2_HUMAN	AIVSLGLLSF	VGFAMGIAG	ISKFLQFQ	LFNEINARK
Q01814-8 / AT2B2_HUMAN	AIVSLGLLSF	VGFAMGIAG	ISKFLQFQ	LFNEINARK

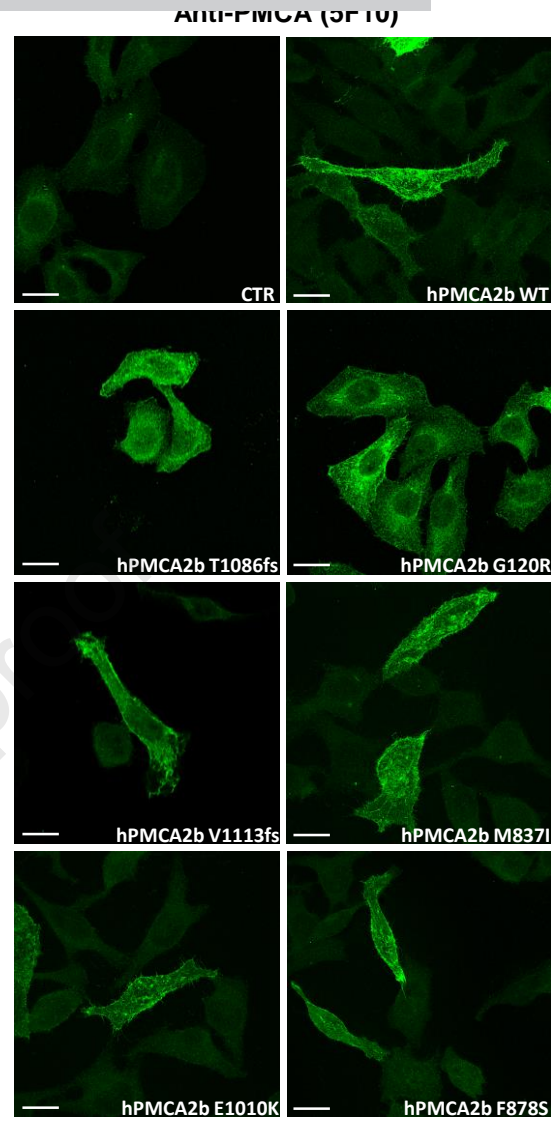




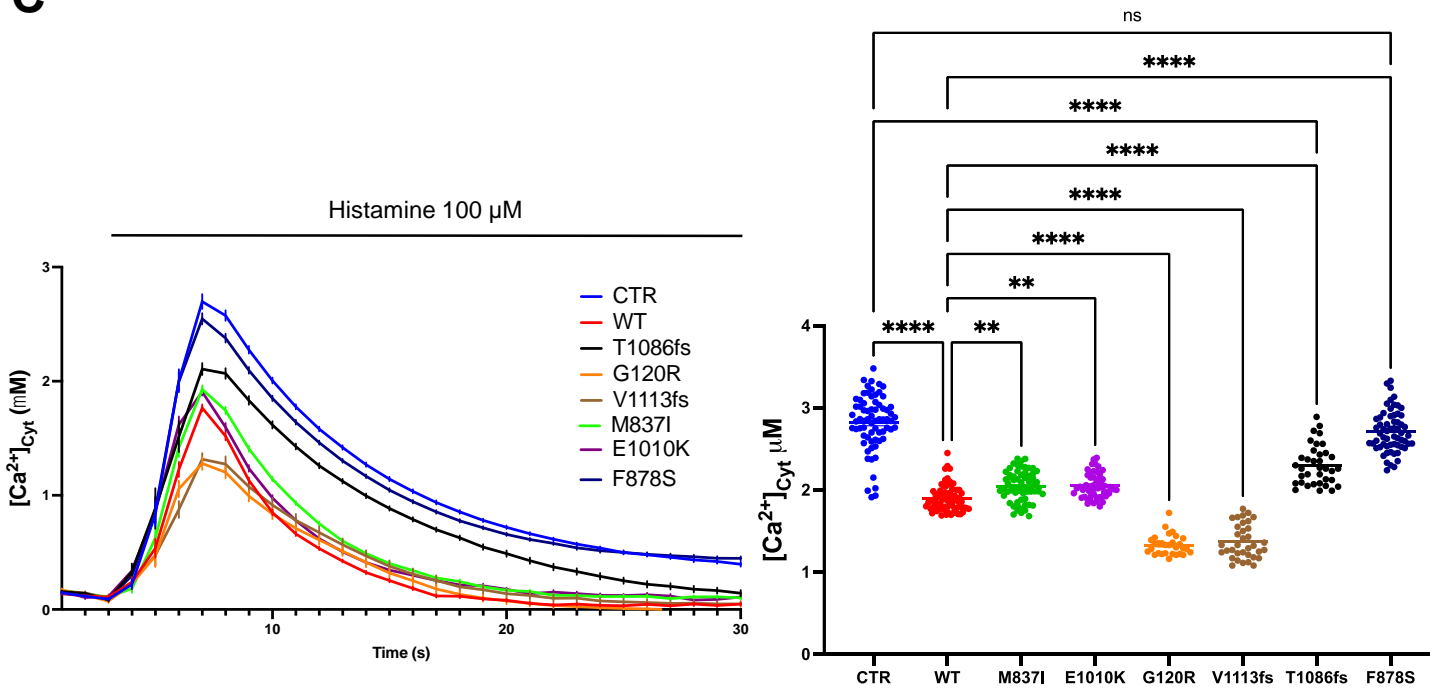
A



B



C



Disclosure: The authors declare no conflict of interest.

Journal Pre-proof